I&EC research
Industrial & Engineering Chemistry Research

ARTICLE

pubs.acs.org/IECR

Additive-Driven Dissolution Enhancement of Colloidal Silica. 2. Environmentally Friendly Additives and Natural Products

Konstantinos D. Demadis,* Eleftheria Mavredaki,† and Maria Somara

Crystal Engineering, Growth and Design Laboratory, Department of Chemistry, University of Crete, Voutes Campus, Heraklion, Crete GR-71003, Greece

Supporting Information

ABSTRACT: The effect of various environmentally friendly chemical additives and natural products on the dissolution of amorphous silica (Aerosil 200 and laboratory-synthesized, SSD) is studied. The silica scale dissolvers tested include the following: ascorbic acid (vitamin C, **ASC**), citric acid (**CITR**), carboxymethyl inulin (**CMI**), 3,4-dihydroxybenzoic acid (catechuic acid, **DHBA**), 3,4,5-trihydroxybenzoic acid (gallic acid, **GA**), dopamine hydrochloride (**DOPA**), iminodiacetic acid (**IDA**), histidine (**HIST**), phenylalanine (**PHALA**), and malic acid (**MAL**). The chemical structures of these chemical additives contain potentially dissolution-active moieties, such as 1,2-dihydroxyethylene (**ASC**), α-hydroxycarboxylate (**MAL** and **CITR**), catecholate (**DHBA**, **GA**, and **DOPA**), α-aminocarboxylate (**HIST** and **PHALA**, both aminoacids), and finally carboxy-modified fructofuranose units (**CMI**). It was found that all studied molecules showed variable dissolution efficiency, with **MAL**, **CMI**, **HIST**, and **PHALA** being the slowest/least effective dissolvers, and the catechol-containing **DHBA**, **GA**, and **DOPA** being the most effective ones. **IDA** and **CITR** have intermediate efficiency.

INTRODUCTION

"Green chemistry" has become a topic of intense discussion and debate during the past decade.[1] The concept of green chemistry has infiltrated all aspects of chemistry and related technological fields. One important area where green chemistry can potentially find several applications is the use of environmentally acceptable additives for water treatment.[2]

Chemical additives are used to condition water so the following problems do not occur, or are minimized:[3] (a) scale formation-deposition of sparingly soluble salts, (b) corrosion of metal surfaces, and (c) development of biofouling.

Naturally, chemicals that are added to condition water have various purposes, and thus dramatically different physicochemical properties. For example, organophosphonates are used to combat calcium/barium/strontium salt formation and deposition.[4] Control of other types of scales, e.g., silica[5] or metal silicates,[6] requires a more thoughtful and at times "exotic" approach. Colloidal silica presents a problem that has been poorly solved and still represents an area of development for inhibitor chemistries.[7]

An important definition of a "green chemical" has been given by Anastas and Warner.[1a] They have given a broad definition of green chemistry based on 12 principles that relate to several steps, from chemical synthesis to chemical usage. A green chemical should be synthesized in a safe and energy efficient manner; its toxicity should be minimal, whereas its biodegradation should be optimal. Lastly, its impact to the environment should be as low as possible.

The OSPAR Commission (*Os*lo and *Par*is Commission[8]) is the international body responsible for harmonization of the strategies and legislation in the North-East Atlantic Region. The Commission has stated that every effort should be made to combat eutrophication and achieve a healthy marine environment where eutrophication does not occur. Chemicals are classified differently depending on the particulars of the geographical area. The guidelines set by OSPAR are the following: (a) biodegradability (>60% in 28 days. When it is < 20%, the chemical is a candidate for substitution), (b) toxicity (LC_{50} or EC_{50} > 1 mg/L for inorganic species, LC_{50} or EC_{50} > 10 mg/L for organic species), and (c) bioaccumulation ($\log_{pow}$ < 3, pow = partition in octanol/water).

When a chemical fulfils two out of three requirements and its biodegradability is superior to 20% in 28 days it is eligible to be listed on the PLONOR List (pose little or no risk). This emphasizes the biodegradability factor and influences usage of water additives.

In part 1 of this series of papers[9] and earlier in a short communication[10] we studied in detail the silica dissolution efficiency at pH 10 of several anionic additives that contain carboxylic or phosphonic acid groups, or both. In this paper we present results on the silica dissolution ability of a number of chemical additives that are natural products, and/or environmentally friendly. Their schematic chemical structures are shown in Figure 1.

There is a plethora of information on these chemicals in a variety of bibliographical sources. In Table 1 we present some essential information on them, which can be a starting point of further research by the reader.

EXPERIMENTAL SECTION

Instruments and Materials. Instruments, reagents, and materials for the silicomolybdate test,[3a,21] the silica dissolution protocol, and interference tests were identical to those used in

Received: August 12, 2011
Accepted: November 9, 2011
Revised: November 9, 2011
Published: November 09, 2011

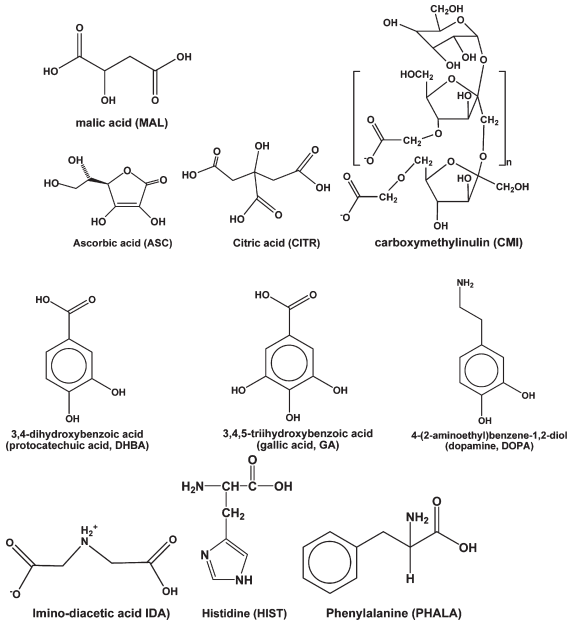

Figure 1. Schematic structures of silica dissolution agents used in this study.

part 1 of this series.[9] All dissolver molecules were purchased from Aldrich Chemical Co. and used as received. CMI solution (available as Dequest-PB11615) was a donation from Thermphos Trading GmbH, Zug, Switzerland. Laboratory-synthesized amorphous silica (SSD) was synthesized as in the preceding paper (part 1).[9] Model colloidal silica is Aerosil 200 from Degussa (water content ~ 1.5%, BET surface area 200 ± 25 m^2/g). The choice of Aerosil 200 was based on its high surface area and absence (by powder X-ray diffractometry) of crystalline phases. Water content for SSD silica was determined to be ~1.5−2.0% (by thermogravimetry) due to rapid surface adsorption of water. BET surface area was measured to be ~100 ± 30 m^2/g.

IR spectra were recorded on an FT-IR Perkin-Elmer FT 1760 in KBr discs. The measurements of soluble silicic acid were performed on a HACH 890 spectrophotometer from the Hach Co., Loveland, CO. SEM images and EDS studies were performed on a scanning electron microscope LEO VP-35 FEM.

Silica Dissolution Protocol. Glass containers must be avoided in order to minimize silica leach-out. A quantity of colloidal silica corresponding to 500 ppm as silica (for 100 mL final solution volume the calculated silica weight is 50 mg) is placed in a polyethylene container together with 80 mL of deionized water and a dosage of specific chemical additive (2500−10 000 ppm, depending on the specific run). We chose to calculate additive dosages based on "ppm" rather than "mg" or "mmol" in order to be consistent with the nomenclature used in the water treatment field. Then, solution pH is adjusted to 10.0 by use of NaOH solution (10% v/v). The specific pH values for dissolution were chosen for the following reasons: (a) this is the maximum operational pH for real water systems that operate without pH control; (b) all dissolution additives are in their deprotonated state at that pH; and (c) preliminary experiments (not reported here) showed that the SiO_2 dissolution rates are too slow for any practical experimental setup. Finally, solutions were diluted up to 100 mL and kept under continuous stirring for a total of 72 h. Soluble silica measurements on small samples withdrawn are made at 24, 48, and 72 h with the silicomolybdate spectrophotometric test.[3a,21] After each measurement pH is again checked, and in the case of pH shift from the target value a readjustment is made. Such deviations were seldom. Dissolution experiments were also run at shorter times (8 h), and sampling was more frequent (every 1 h).

Dissolver Interference Test. Every cleaning additive is tested for its interference with the silicomolybdate spectrophotometric test. A stock solution (500 ppm, expressed as "ppm SiO_2") of soluble silica (prepared from commercial sodium silicate) is prepared by dissolving 4.4 g of $Na_2SiO_3 \cdot 5H_2O$ in 2.5 L of nanopure water. The pH of the above solution was 11.50. To 100 mL of that solution a dosage of the cleaning chemical is added (2500−10 000 ppm). After appropriate dilutions are made, soluble silica is measured with the silicomolybdate spectrophotometric test.[19] The results are compared to the expected value of 500 ppm. From the additives tested **GA** and **DOPA** showed unacceptable interference and were treated differently (see below).

Silica Scale Dissolution from a Stainless Steel Surface. *Silica Deposition.* Colloidal silica was first deposited on a stainless steel coupon, as follows. A quantity of $NaSiO_3 \cdot 5H_2O$ (2 g) was dissolved in 100 mL of deionized water. The pH of the solution was adjusted to 7.0 ± 0.1 by addition of 80% v/v HCl solution under vigorous stirring. Immediately after pH adjustment a preweighted stainless steel specimen (coupon) was immersed into the solution. The setup was allowed to stand for 72−168 h in order to allow silica to deposit on the steel surface. The steel specimen was then withdrawn and left to air-dry. Its weight was again remeasured, and by difference, the amount of deposited amorphous silica was calculated. This procedure was repeated before each dissolution experiment, described below.

Dissolution of Deposited Silica. For the dissolution experiment, a 100 mL solution of the desired dissolver was prepared in a PET container, containing various amounts of dissolver (2500−10 000 ppm). The fouled stainless steel specimen (prepared as above) was then immersed into the solution, the container was covered with parafilm, and the solution was kept under gentle stirring (in order to avoid mechanical dislodging of the deposited scale) at pH 10. The dissolution experiment was left to proceed for a specified time period (3−7 days, depending on the experiment, see Table 2 for details of each additive), after which the specimen was withdrawn, left to air-dry, and weighted. From the difference in weight of the "fouled" and the "cleaned" specimen, the dissolution performance of each dissolver was quantified.

■ RESULTS AND DISCUSSION

Effect of Additives on Aerosil 200 Silica Dissolution during "Long-Term" Experiments. In the experiments described herein, stirred suspensions containing colloidal silica and the dissolution additive at various concentrations are vigorously stirred at a fixed pH of 10 and then tested for soluble silica by the silicomolybdate spectrophotometric method[21] after 24, 48, and 72 h (long-term experiments), or every hour for 8 h (short-term experiments) of dissolution time.

The results of silica dissolution in the presence of silica dissolvers are presented in Figure 2. The measurement methodology followed for silica is based on the quantification of "soluble" (or "reactive") silica after dissolution experiments are performed for at least 24 h. Colloidal silica is completely unreactive to the silicomolybdate spectrophotometric test.

After 24 h, in "control" solutions (no additive present) dissolution proceeds until ~120 ppm silica is solubilized (~24%). The "% solubilized silica" is calculated as [("ppm soluble silica")/500] × 100. The number "500" indicates the initial silica level of 500 ppm.

Table 1. Chemical Additives Used in This Study: Occurrence and Properties.

additive abbreviation	IUPAC name	natural occurrence	toxicity	miscellaneous attributes/properties	ref
MAL	hydroxybutanedioic acid	most unripe fruits, apple juice, grapes, intermediate in citric acid cycle	none; however, excessive consumption can cause irritation of the mouth, and no tolerable upper level intake (UL) has been established	pK_{a_1} = 3.40, pK_{a_2} = 5.20	11
ASC	(5*R*)-[(1*S*)-1,2-dihydroxyethyl]-3,4-dihydroxyfuran-2(5H)-one	fruits and vegetables, meat, especially liver, mother's milk	none; however, relatively large doses of ascorbic acid may cause skin rashes, indigestion, nausea, vomiting, diarrhea, flushing of the face, headache, fatigue and disturbed sleep	antioxidant and antiscorbutic properties	12
CITR	2-hydroxypropane-1,2,3-tricarboxylic acid	citrus fruits	diarrhea, loose stools, nausea, upset stomach, vomiting, enamel damage; oral (LD_{50}) acute: 5040 mg/kg (mouse); 3000 mg/kg (rat)	metal chelant, pK_{a_1} = 3.09, pK_{a_2} = 4.75, pK_{a_3} = 6.41	13
CMI	not available	none; it is produced from inulin by a carboxymethylation process, and inulin is found in chicory roots (∼18% dry content) and in onion, garlic, and agave.	oral rat toxicity >2000 mg/kg B.W., subacute toxicity 28 days (rat) 1000 mg/kg B.W., no mutagenicity in Ames test, no dermal sensitization on guinea pigs	metal chelator, mineral scale inhibitor	14
DHBA	3,4-dihydroxybenzoic acid (protocatechuic acid)	natural phenolic compound found in many edible and medicinal plants, e.g., Roselle plants (*Hibiscus sabdariffa*)	induces apoptosis of human leukemia cells, as well as malignant HSG1 cells taken from human oral cavities	antioxidant, protective agent against cardiovascular diseases and neoplasms: pK_{a_1} 4.48 (COOH), pK_{a_2} 7.86, pK_{a_3} 13.22 (OH)	15
GA	3,4,5-trihydroxybenzoic acid	gallnuts, sumac, witch hazel, tea leaves, oak bark, and other plants	acute oral toxicity (LD_{50}): 5000 mg/kg (rabbit)	commonly used in the pharmaceutical industry and can also be used to synthesize the hallucinogenic alkaloid mescaline; inhibits liver metastasis; also used to treat albuminuria and diabetes, and possesses antifungal and antiviral properties: pK_{a_1} 4.09 (COOH), pK_{a_2} 7.3, pK_{a_3} 12.17 (OH)	16
DOPA	4-(2-aminoethyl)benzene-1,2-diol	biosynthesized in the body (mainly by nervous tissue and the medulla of the adrenal glands) from tyrosine	LD_{50} oral (mice) = 1460 mg/kg, LD_{50} oral (rats) = 1780 mg/kg	it has many functions in the brain, including important roles in behavior and cognition, voluntary movement, motivation, punishment and reward, inhibition of prolactin production (involved in lactation and sexual gratification), sleep, mood, attention, working memory, and learning	17
IDA	2-(carboxymethylamino)acetic acid		intraperitoneal (mouse) LD_{50}: 250 mg/kg, low persistence in water/soil, low bioaccumulation	metal chelator, used in the hydroxyiminodiacetic acid (HIDA) scan, which is a test to show proper function of liver and gallbladder. pK_{a_1} 2.98, pK_{a_2} 9.89	18

dx.doi.org/10.1021/ie201798e |*Ind. Eng. Chem. Res.* 2011, 50, 13866–13876

Table 1. Continued

additive abbreviation	IUPAC name	natural occurrence	toxicity	miscellaneous attributes/properties	ref
HIST	2-amino-3-(1*H*-imidazol-4-yl)propanoic acid	plant proteins found in rice, wheat, rye and other cereals, also found in abundance in all dairy products, meats and poultry as well as fish together with other amino acids; other sources include radishes, carrots, cucumber, beetroots, celery, garlic, onions, turnips, alfalfa, spinach, pineapples, apples, pomegranates, papaya	not carcinogenic in F344 rats at doses 2.5% of their diet for 104 weeks	essential amino acid in humans and other mammals: pK_a values 1.82 (carboxylic acid), 6.04 (pyrrole NH), and 9.17 (ammonium NH)	19
PHALA	2-amino-3-phenylpropanoic acid	found in almonds, avocado, bananas, cheese, lima beans, nonfat dried milk, peanuts, pickled herring, pumpkin seeds, sesame seeds	PHALA doses in excess of 5000 mg/day may be toxic and can cause nerve damage; high quantities of *DL*-phenylalanine may also cause mild side effects such as nausea, heartburn, and headaches	precursor for tyrosine, the monoamine signaling molecules dopamine, norepinephrine (noradrenaline), and epinephrine (adrenaline), and the skin pigment melanin: pK_a values 1.83 (carboxyl), 9.13 (amino)	20

Silica dissolution continues after 48 and 72 h allowing soluble silica levels to increase to ~150 ppm (~30%) and ~190 ppm (~38%), respectively. These results obtained for silica dissolution in the absence of any additives need to be surpassed by satisfactorily performing additives. Examination of Figure 2 shows that additives **CMI**, **PHALA**, and **MAL** are mildly effective silica dissolvers, within the timeline of the experiments (3 days). In the case of **CMI** only the 2500 ppm dosage is somewhat effective (~250 ppm silica dissolution). Soluble silica levels in the presence of higher dosages of **CMI** are virtually the same as those in "control" solutions. The same behavior is noted for **MAL**. The dissolution efficacy of **PHALA** steadily increases up to 7500 ppm dosage, achieving ~300 ppm silica dissolution. This behavior is comparable to that of **HIST**.

IDA induces dissolution of 318 ppm silica (for the 2500 pm dosage after 72 h). Its performance slightly increases to 338 ppm (for the 5000 pm dosage after 72 h), and 327 ppm (for the 7500 pm dosage after 72 h). The hydroxyl-tricarboxylate **CITR** shows rather low efficiency for dosages <7500 ppm, but proves to be a satisfactory dissolver at 10 000 ppm, dissolving nearly 400 ppm of silica.

Of the additives containing the catecholate moiety (**DHBA**, **GA**, and **DOPA**), only **DHBA** could be used in experiments which involved soluble silica quantification by the silicomolybdate test. The experiments with **GA** and **DOPA** were treated differently (see below).

DHBA is a very efficient silica dissolution agent. Although it only dissolves ~250 ppm silica at 2500 ppm dosages (within 24 h), its efficiency steadily improves at higher dosages. For example, it dissolves ~385 ppm (at 5000 ppm within 24 h), 470 ppm (at 7500 ppm within 24 h), and 480 ppm silica (at 10 000 ppm within 24 h). It is observed that, for a given dosage, solubilized silica steadily drops after 24 h. For example, for 7500 ppm dosage, soluble silica is 472 ppm after 24 h, 404 ppm after 48 h, and 360 ppm after 72 h. A possible explanation for this could be the instability of the putative "Si-DHBA complex", which may revert to silicic acid, which in turn can be reincorporated into the colloidal silica particles. Some relevant comments are made later in the short literature review section.

Effect of Additives on Silica Dissolution during "Short-Term" Experiments. From the additives presented above, we selected **DHBA** and **HIST** for further study. These were selected in order to compare dissolution performance of an "effective" (**DHBA**) and a "mediocre" (**HIST**) dissolver during the first stages of silica dissolution. Thus, **DHBA** and **HIST** were studied in "short-term" silica dissolution experiments, in which solution sampling was done every hour for the first 8 h of the dissolution reaction. The results are shown in Figure 3.

The results obtained for **DHBA** nicely demonstrate that there is a clear dose−response relationship in its dissolution efficiency within the first 8 h of reaction. Although differentiation in silica dissolution among the various **DHBA** dosages is not very clear in the first stages of the experiment (<3 h), this becomes evident as dissolution time proceeds. In the case of **HIST** (a "poorer" silica dissolver), differentiation between the efficiency for various dosages is nearly impossible, even at the end of the 8 h period.

In order to carry out a more useful comparison between the various additives, a graph can be constructed that presents the dissolution efficiency of all additives. Dissolution efficiency is defined as follows:

$$\text{Dissolution Efficiency}(\%) = \frac{(A - C)}{(500 - C)} \times 100$$

Here, A = measured soluble silicic acid at 72 h (in ppm) after dissolution by an additive at 5000 ppm dosage, and C = measured

Table 2. Dissolution of Silica-Fouled Stainless Steel Surfaces by Various Dissolvers

dissolution agent	dissolver dosage (ppm)	fouled surface	silica scale removed (mg)	dissolution time (h)	dissolution rate[a]	% dissolution efficiency[b]
control (no dissolver)		stainless steel	7.0	96	0.073	54
carboxymethyl inulin (CMI)	2500	stainless steel	20.0	96	0.208	68
carboxymethyl inulin (CMI)	5000	stainless steel	24.0	96	0.250	77
carboxymethyl inulin (CMI)	10 000	stainless steel	74.0	96	0.771	94
histidine (HIS)	10 000	stainless steel	108.0	168	0.643	94
phosphonobutane-1,2,4-tricarboxylic acid (PBTC)	5000	stainless steel	24.0	96	0.250	96
phosphonobutane-1,2,4-tricarboxylic acid (PBTC)	10 000	stainless steel	145.0	168	0.863	~100
ascorbic acid (ASC)	5000	stainless steel	28.0	72	0.389	78

[a] Calculated as "mg scale/h". [b] Dissolution efficiency is calculated as follows:

$$\frac{\text{weight of fouled specimen} - \text{weight of cleaned specimen}}{\text{weight of fouled specimen}}$$

soluble silicic acid at 72 h (in ppm) after dissolution for the "control" (no additive present).

The results of such calculation are presented in Figure 4.

Differences in Dissolution between Aerosil 200 and SSD Silica. We investigated how the nature of silica (commercial or laboratory-synthesized) affects dissolution efficiency. Thus, we compared the dissolution efficiency of **DHBA**, **CMI**, and **IDA** on two kinds of silica, Aerosil 200 and SSD silica. Silica dissolution protocols were the same as in part 1.[9] Solubilized silica was quantified by the silicomolybdate test.[3a,10,21] The results are given in Figure 5, and the comparison is quite revealing. SSD silica is poorly responsive to dissolution in the absence of any additives at pH 10. In fact, after 24 h only ~90 ppm are dissolved, in comparison to dissolution of ~130 ppm of Aerosil 200 under the same conditions. As a general trend, SSD was much less responsive to dissolution induced by **DHBA**, **CMI**, and **IDA**. For **CMI** and **IDA**, the levels of soluble silica never exceeded those for the "control". However, for **DHBA** dissolution efficiency was systematically higher than that for the "control" in SSD silica dissolution. The best-performing dosage for **DHBA** was 10 000 ppm, which dissolves nearly 250 ppm SSD silica after 72 h.

The textural features of SSD silica are most likely responsible for the fact that it is recalcitrant to dissolution. As shown in part 1,[9] SSD particles appear dense and compact, in contrast to those of Aerosil 200. The surface area of Aerosil 200 is approximately double that of SSD silica. Therefore, the particle coverage in the case of Aerosil 200 is much more effective than that of SSD silica. In both cases additives cannot penetrate into the particle, but can only achieve dissolution through surface interactions.

Dissolution of Silica Deposits from a Fouled Stainless Steel Surface. Inorganic foulants are most commonly found deposited on critical equipment surfaces. Hence, there are times where system operators are called upon removing foulants deposited on surfaces. In this context, and in order to evaluate the ability of selected dissolvers to dissolve silica deposited onto a surface, we followed the following approach. Colloidal silica was prepared *in situ* and was deposited onto a stainless steel surface as described before.[9] The selection of stainless steel as the fouled surface was based on the fact that it is not susceptible to metallic corrosion, an event that complicates silica deposition.[22] The fouled specimens were then removed, air-dried, and weighed. Some of them were characterized by SEM in order to study the texture of the silica deposit. The specimens were then subjected to a dissolution process in the presence of various additives. For this particular study we selected the additives **CMI**, **HIS**, **ASC**, and **PBTC**. **CMI** is a "green" polymer, **HIS** is an aminoacid, **ASC** is a vitamin, and **PBTC** is a very effective silica dissolver (studied in detail in part 1).[9,10] At the end of the specified dissolution time, the specimens were removed, air-dried, and weighed. Dissolution efficiency was determined by the weight difference. Selected cleaned specimens were studied by SEM, in order to visualize dissolution efficiency. The results are given in Table 2.

The stainless steel surfaces were examined by SEM after silica deposition (Figure 6, upper image), after dissolution in the absence of any additives (control, Figure 6, middle image), and after chemical cleaning by CMI (Figure 6, lower image). A clear dissolution effect is demonstrated by comparison of the three images. EDS was performed on the silica fouled surface (Figure 6, upper image) and showed presence of pure silica (Si/O ratio ~ 1:2), see Supporting Information (SI) Figure S-1. EDS of the steel surface after the dissolution experiment in the presence of CMI (Figure 6, lower image) showed the presence of Fe only, see SI Figure S-2. The small white areas on the Fe surface are leftover attached silica scale.

Silica Dissolvers with a Catechol Functionality. Three silica dissolvers contain the catechol (1,2-dihydroxybenzene) functionality in their backbone (protocatechuic acid, **DHBA**; gallic acid, **GA**; and dopamine, **DOPA**). Before testing them in dissolution experiments, their UV−vis spectra were collected at neutral and strongly alkaline pH regions, in order to ascertain whether they absorb around the region of 450 nm (needed for the soluble silica determination by the silicomolybdate method). In Figure 7, the UV−vis spectrum in aqueous solutions of pH 7, 9, and 10 of **DOPA** is shown.

It becomes evident that quantification of silica dissolution in the presence of **DOPA** is not possible spectrophotometrically. Similar observations were noted for gallic acid (**GA**).[23] **DHBA** did not absorb in the region of interest,[24] and its dissolution efficiency was studied as the other dissolvers. For the dissolvers **DOPA** and **GA**, a different approach was followed. Dissolution efficiency was measured on the basis of the weight difference of the solid silica before and after the dissolution. The results for **DOPA** (pH 10.0 and 2500−10 000 levels) and **GA** (pH 7.0 and 9.0, and 1000−5000 levels) are shown in Figure 8.

DOPA exhibits a clear dosage-dependent behavior. Its dissolution efficiency increases almost linearly as dosage increases from 2500 ppm to 10 000 ppm. At the highest dosage it reaches quantitative silica dissolution. **GA** appears to be an effective

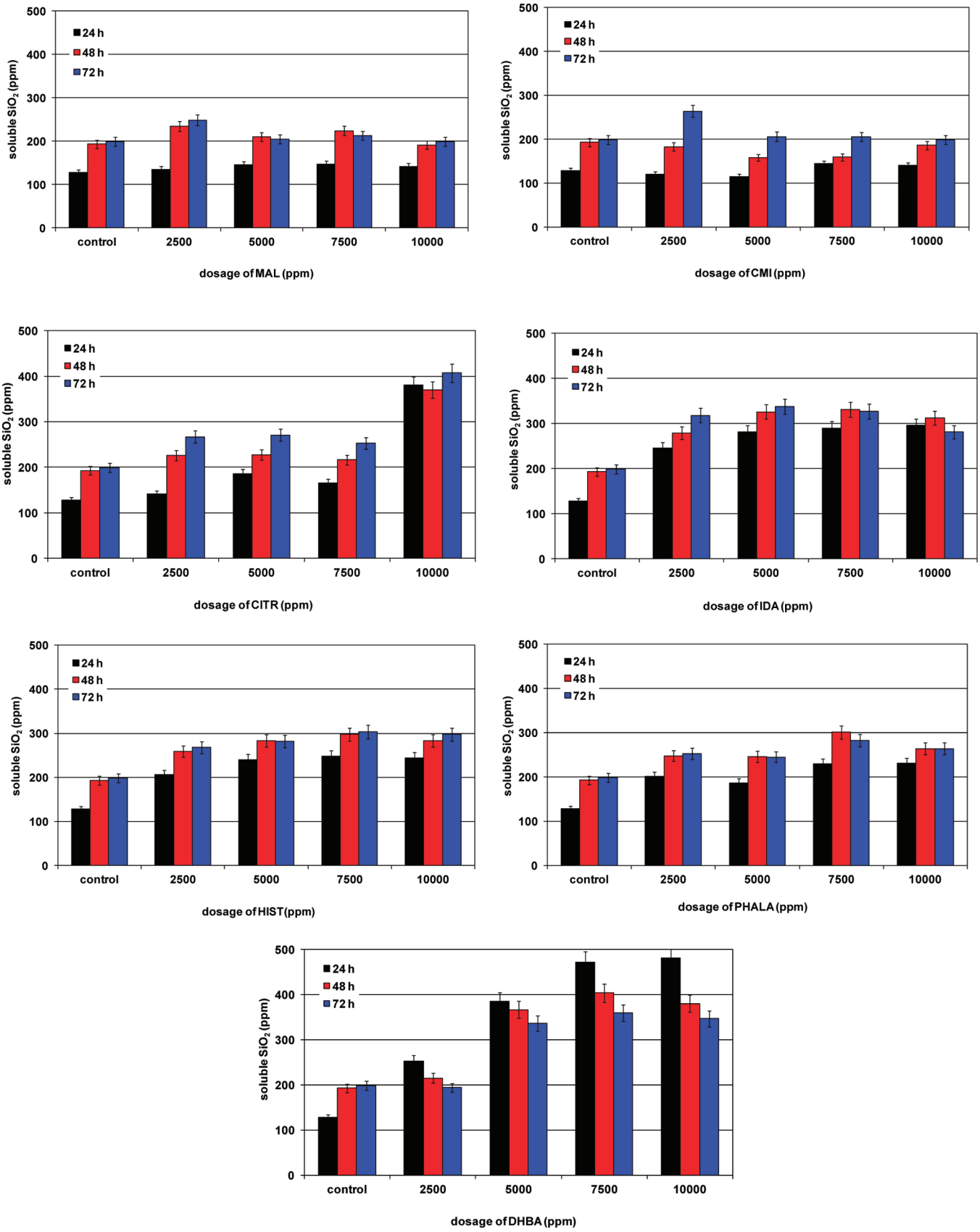

Figure 2. Dose−response graphs of silica dissolution experiments for various additives, as indicated.

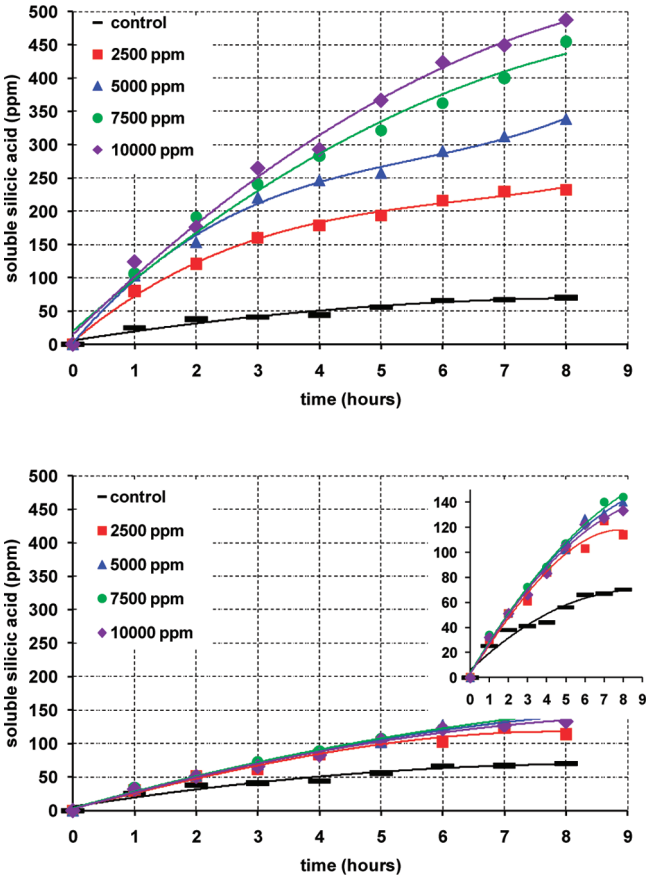

Figure 3. Silica dissolution by **DHBA** (upper) and **HIST** (lower) during the first stages (8 h).

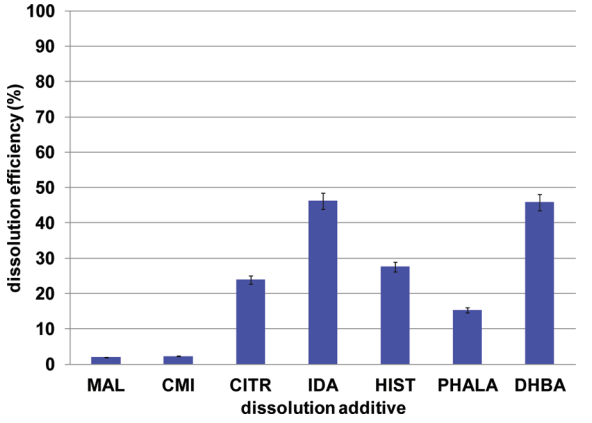

Figure 4. Dissolution efficiency for the additives tested in this work.

dissolver in both studied pH values (7 and 9). At sufficiently high dosages it reaches nearly quantitative dissolution. This undoubtedly is related to the readily formed, stable chelating rings of the catecholate functionality with the Si center. A more in-depth discussion on possible mechanisms will follow below.

Characterization of Silica Dissolution by Scanning Electron Microscopy (SEM). The morphology of the silica particles that underwent the dissolution process in the presence of **GA** was evaluated by SEM, and the results can be compared to those from authentic samples of Aerosil 200 and SSD (before and after dissolution). The images are presented in Figures 9−11. In Figure 9,

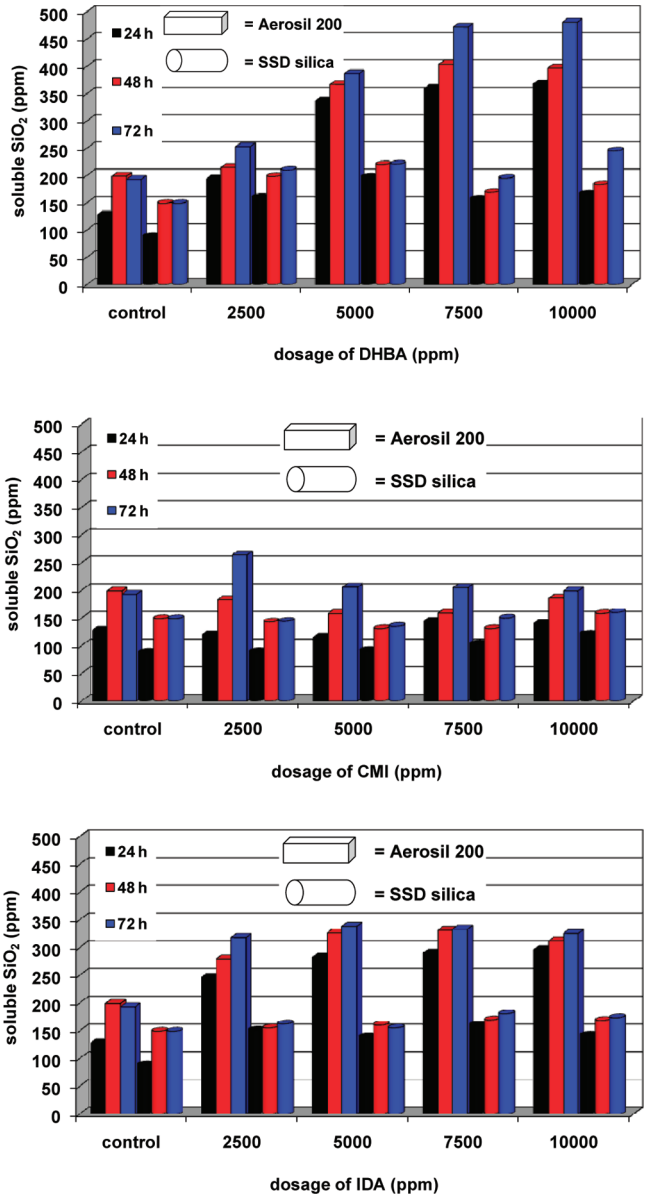

Figure 5. Comparison of dissolution efficiency of **DHBA**, **CMI**, and **IDA** on two kinds of amorphous silica: parallelepipeds, Aerosil 200; cylinders, SSD silica.

we present SEM images that reveal the morphology of neat silica particles of Aerosil 200 (Figure 9, upper) and SSD (Figure 9, lower) before dissolution. The images show that silica particles are loose aggregates of sizes <50 nm in the case of Aerosil 200. For SSD the particles are obviously larger than those for Aerosil 200 and show severe aggregation forming fairly uniform films.

The above silica particles were subjected to a dissolution experiment without any additives ("control") at pH 7, for 24 h, and the images of the undissolved particles are shown in Figure 10. No dramatic differences were noted, neither in particle size nor in particle morphology. These results are consistent with the dissolution results for the "control" shown in Figure 8 (middle), which shows that less than 5% dissolution takes place.

Silica particles that were exposed to solutions containing **GA** (2000 ppm dosage, at pH 7 for 24 h) were studied by SEM. The images are presented in Figure 11. For the Aerosil 200 silica

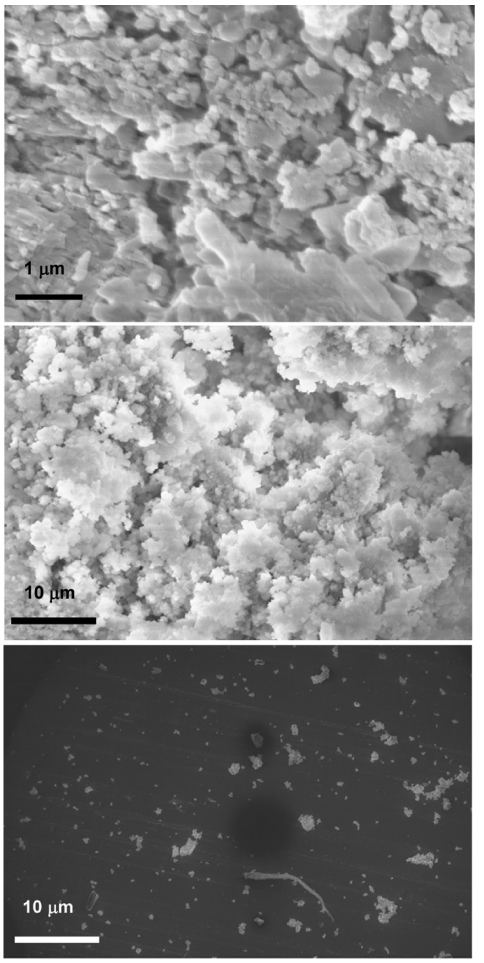

Figure 6. SEM image of the silica fouled stainless steel specimen (upper). Specimen exposed to a pH 10 solution in the absence of additives (middle). Cleaned specimen after exposure to a solution containing 10 000 ppm CMI (lower). Exposure time is 96 h (see Table 2).

particles (Figure 11, two upper images) there are notable differences in the morphology of the undissolved precipitates. First, the silica particles appear very compact (Figure 11, upper left image), and their appearance resembles that of a continuous film. The magnified image (Figure 11, upper right image) reveals that the particles are ~30 nm in size and are smaller in size than the ones from neat Aerosil 200 particles either before (Figure 9, upper right image) or after (Figure 10, upper right image) dissolution (in the absence of additives). The observation that the particles now show enhanced aggregation and size is a strong indication that **GA** is incorporated within the precipitate. Corroborating evidence comes from FT-IR studies that showed the presence of an intense ν(C═O) asymmetric stretch centered at ~1600 cm^{-1}, see SI Figure S-3. This shows the presence of a deprotonated carboxylic acid group ($-COO^-$) in the silica precipitate. For comparison, the ν(C═O) asymmetric stretch for **GA** appears at ~1700 cm^{-1}, see SI Figure S-4, consistent with the presence of a protonated carboxylic acid ($-COOH$) moiety.[25] The pH = 7 of the dissolution experiment is sufficiently high to cause deprotonation of the $-COOH$ group.[26] Similar observations can be put forth for the SSD silica particles exposed to GA, under the same conditions (Figure 11, two lower images). Again, the silica particles exhibit severe aggregation and form continuous films (lower left image), although the films appear

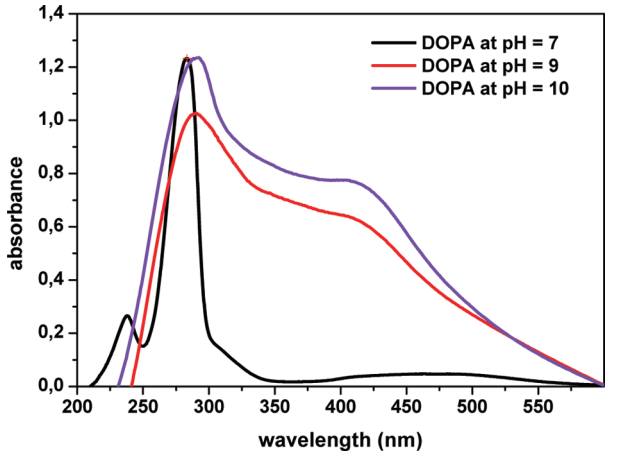

Figure 7. UV−vis spectra of **DOPA** in different pH regions of interest.

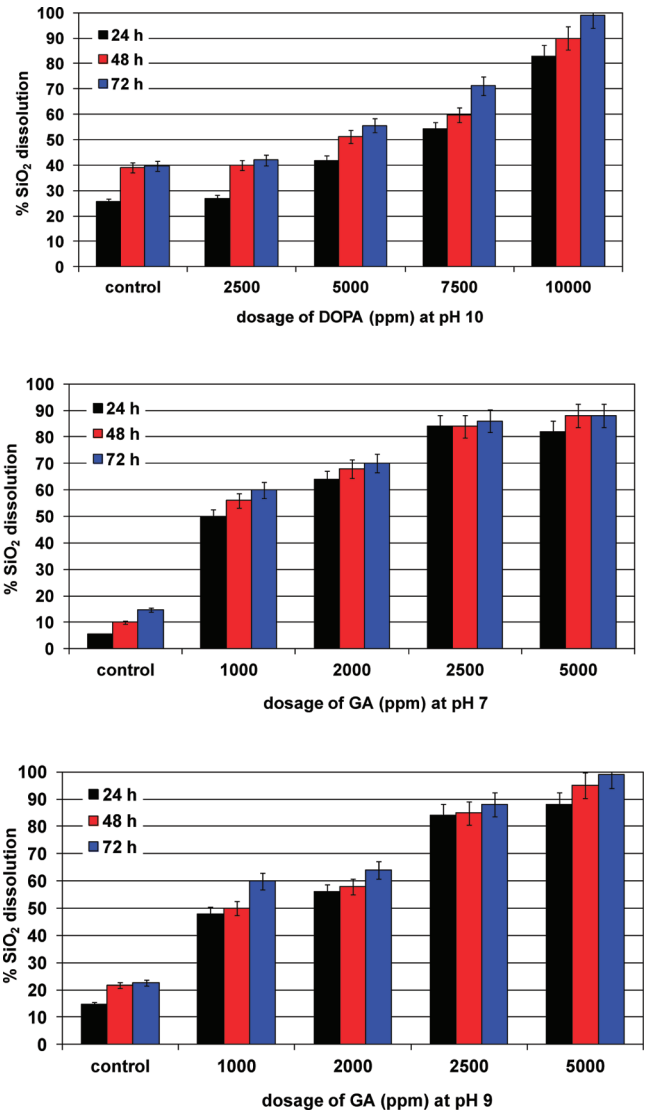

Figure 8. Dissolution of silica (%) in the presence of various levels of dopamine (**DOPA**, pH 10, upper), and gallic acid (**GA**, pH 7, middle; pH 9, lower).

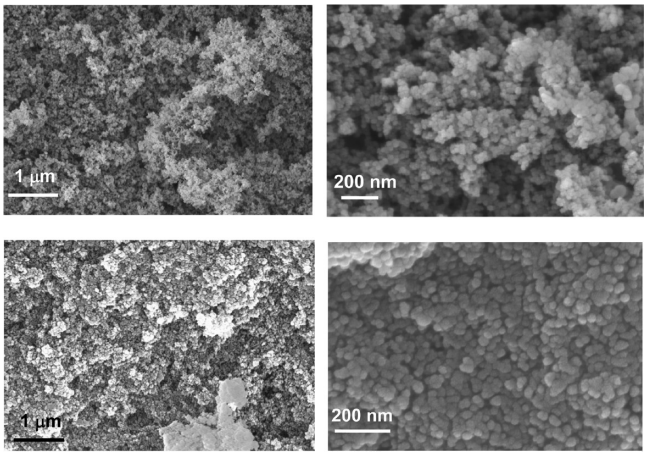

Figure 9. SEM images of neat silica particles (before dissolution) from Aerosil 200 (two upper images) and synthetic SSD silica (two lower images).

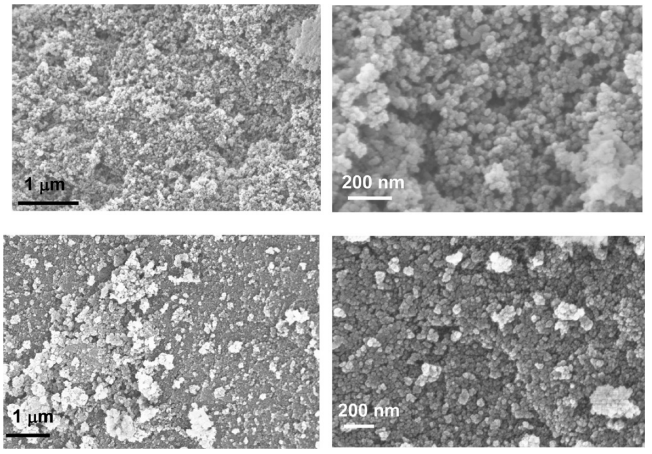

Figure 10. SEM images of silica particles after dissolution at pH 7 for 24 h from Aerosil 200 (two upper images) and synthetic SSD silica (two lower images), in the absence of any additives.

"rougher" than those for Aerosil 200 silica. Under higher magnification (lower right image) the tendency for aggregation is further revealed. It is worth noting that, upon closer examination of the aggregated particles, it becomes apparent that they are composed of even much smaller elementary particles of subnanometer size.

Short Literature Review on Silica Dissolution by Catecholate-Type Dissolvers. Silica dissolution in natural and artificial environments has been reviewed recently.[27] The interactions between complexing agents and metal oxide surfaces are well established.[28] Herein we present some relevant results pertaining to catecholate-type molecules taken from the literature.

Recently, Rao et al. studied a plethora of biocompatible molecules, such as imidazole, histidine, lysine, glutamic acid, glycine, glutamine, 1-*N*-hydroxyimidazole-3-*N*-oxide, 3,4-dihydroxy phenylalanine, and myo-inositol, in silica dissolution and subsequent silicic acid stabilization.[29] They found that histidine and alanine were effective silica dissolvers, among others. Their research was inspired by the discovery that replacement of Lsi1 gene (responsible for silicon uptake in the plant) in rice has resulted in vastly reduced silicon intake, high susceptibility of the leaves to pests, infection of the panicle, and reduction of the yields of crops by 90%.[30]

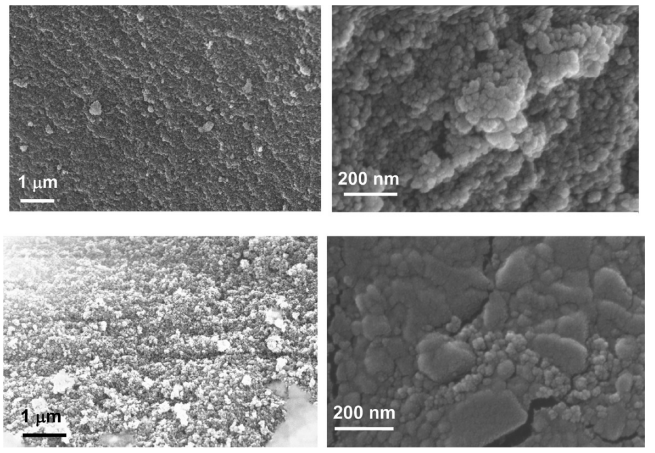

Figure 11. SEM images of silica particles after dissolution in the presence of 2000 ppm gallic acid at pH 7 for 24 h from Aerosil 200 (two upper images) and synthetic SSD silica (two lower images).

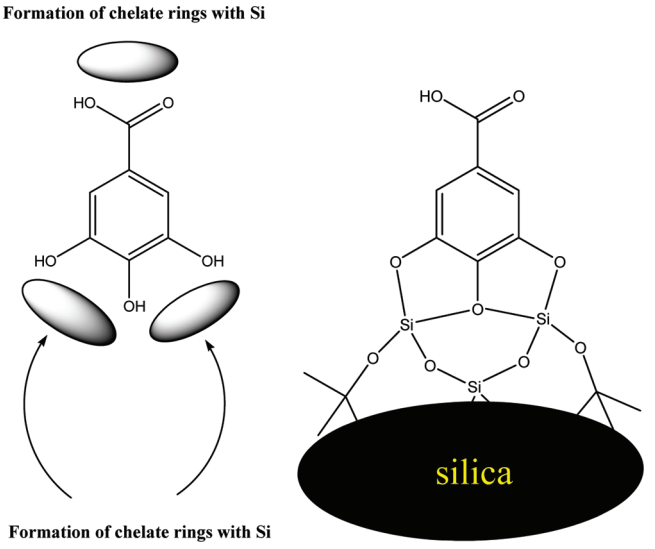

Figure 12. Schematic representation of the stable chelating rings that form in the case of **GA**.

Bai et al. were able to detect a complex with hexacoordinate silicon containing catechol. The identification was done by NMR. This complex is produced by the direct reaction of amorphous silica with catechol.[31] Although such complexes have been reported to be stable in the pH region from 6 to 10,[32] their partial rehydrolysis to free silicic acid may be possible. One can then envision its reincorporation into the undissolved amorphous silica matrix. Perhaps this is happening in the case of **DHBA** (bottom bar graph in Figure 2), where a slight reduction of molybdate-reactive silicic acid is noted.

The adsorption isotherms of catechol (1,2-dihydroxybenzene) and gallic acid onto titanium dioxide (Degussa P-25) were measured at various pH values and room temperature using attenuated total reflection Fourier transform infrared (FTIR-ATR) data.[33] The authors found out that the affinity of these molecules for the TiO_2 surface is largely pH independent, although the deprotonation of the carboxylic group in gallic acid might produce a slight increase in the affinity.

CONCLUSIONS/OUTLOOK

Our research efforts in controlling silica deposits are dual. They involve use of chemical additives to inhibit silica formation, thus stabilizing mono- or disilicic acid.[34] The alternative approach is the use of chemical additives to dissolve/remove silica deposits.[9,10] In this paper, we presented silica dissolution results with several "green" additives and natural products, such as ascorbic acid (vitamin C, **ASC**), citric acid (**CITR**), carboxymethyl inulin (**CMI**), 3,4-dihydroxybenzoic acid (catechuic acid, **DHBA**), 3,4,5-trihydroxybenzoic acid (gallic acid, **GA**), dopamine hydrochloride (**DOPA**), iminodiacetic acid (**IDA**), histidine (**HIST**), phenylalanine (**PHALA**), and malic acid (**MAL**). It was found that all studied molecules showed variable dissolution efficiency, with **MAL**, **CMI**, **HIST**, and **PHALA** being the slowest/least effective dissolvers, and the catechol-containing **DHBA**, **GA**, and **DOPA** being the most effective ones. **IDA** and **CITR** had intermediate efficiency.

The silica dissolution efficiency of additives bearing the catechol functionality can be rationalized by the stable chelating rings that form with the silicon atom, see Figure 12.

Such species have been described in the literature.[28−32] It is conceivable that the initial stage of silica dissolution is surface complexation of catechol-bearing additives (**DOPA**, **GA**, **DHBA**) with silanol groups. Such an interaction weakens the attachment of surface silicon atoms to the silica particle, thus rendering its detachment (by the action of additional additive molecules) more facile.[28−32]

ASSOCIATED CONTENT

Supporting Information. EDS and FT-IR spectra. This material is available free of charge via the Internet at http://pubs.acs.org.

AUTHOR INFORMATION

Corresponding Author

*E-mail: demadis@chemistry.uoc.gr.

Present Address

[†]Institute of Engineering Thermofluids, Surfaces and Interfaces, School of Mechanical Engineering, University of Leeds, England.

ACKNOWLEDGMENT

We acknowledge the Department of Chemistry, University of Crete, the GSRT (Contract GSRT-2006-170c) for partial financial support, and the reviewers for contributing to the improvement of the final manuscript.

REFERENCES

(1) (a) Anastas, P.T.; Warner, J.C. *Green Chemistry: Theory and Practice*; Oxford University Press: New York, 1998. (b) Useful information on green chemistry can be found in the U.S. Environmental Protection Agency web page at http://www.epa.gov/greenchemistry (accessed August 10, 2011). (c) Several principles of green chemistry are analyzed in relevant web sites, see for example http://www.greenchemistry.ca (accessed August 10, 2011), http://portal.acs.org/portal/PublicWebSite/greenchemistry/index.htm (accessed August 10, 2011), and http://www.greenchemistrynetwork.org (accessed August 10, 2011). (d) Einav, R.; Harussi, K.; Perry, D. The footprint of the desalination processes on the environment. *Desalination* **2002**, *152*, 141–154.

(2) (a) Hasson, D.; Shemer, H.; Sher, A. State of the art of friendly "green" scale control inhibitors: A review article. *Ind. Eng. Chem. Res.* **2011**, *50*, 7601–7607. (b) Saleah, A. O.; Basta, A. H. Evaluation of some organic-based biopolymers as green inhibitors for calcium sulfate scales. *Environmentalist* **2008**, *28*, 421–428.

(3) (a) Demadis, K. D.; Mavredaki, E.; Stathoulopoulou, A.; Neofotistou, E.; Mantzaridis, C. Industrial water systems: Problems, challenges and solutions for the process industries. *Desalination* **2007**, *213*, 38–46. (b) Demadis, K. D. Combating heat exchanger fouling and corrosion phenomena in process waters. In *Compact Heat Exchangers and Enhancement Technology for the Process Industries*; Shah, R. K., Ed.; Begell House Inc.: New York, 2003; pp 483−491. (c) Demadis, K. D. Silica scale inhibition relevant to desalination technologies: Progress and recent developments. In *Desalination Research Progress*; Delgado, D. J., Moreno, P., Eds.; Nova Science Publishers, Inc.: New York, 2008; Chapter 6, pp 249−259. (d) Demadis, K. D.; Öner, M. Inhibitory effects of "green" additives on the crystal growth of sparingly soluble salts. In *Green Chemistry Research Trends*; Pearlman, J. T., Ed.; Nova Science Publishers: New York, 2009; Chapter 8, pp 265−287.

(4) (a) Abdel-Aal, N.; Sawada, K. Inhibition of adhesion and precipitation of $CaCO_3$ by aminopolyphosphonate. *J. Cryst. Growth* **2003**, *256*, 188–200. (b) Demadis, K. D.; Katarachia, S. D. Metal-phosphonate chemistry: preparation, crystal structure of calcium-amino-*tris*-methylene phosphonate and $CaCO_3$ inhibition. *Phosphorus Sulfur Silicon* **2004**, *179*, 627–648. (c) Demadis, K. D.; Baran, P. Chemistry of organophosphonate scale growth inhibitors: Two dimensional, layered polymeric networks in the structure of tetrasodium 2-hydroxyethyl-amino-bis(methylenephosphonate). *J. Solid State Chem.* **2004**, *177*, 4768–4776. (d) Demadis, K. D.; Raptis, R. G.; Baran, P. Chemistry of organophosphonate scale growth inhibitors: 2. Structural aspects of 2-phosphonobutane-1,2,4-tricarboxylic acid monohydrate (PBTC·H_2O). *Bioinorg. Chem. Appl.* **2005**, *3*, 119–134. (e) Demadis, K. D.; Lykoudis, P. Chemistry of organophosphonate scale growth inhibitors: 3. Physicochemical aspects of 2-phosphonobutane-1,2,4-tricarboxylate (PBTC) and its effect on $CaCO_3$ crystal growth. *Bioinorg. Chem. Appl.* **2005**, *3*, 135–149. (f) Demadis, K. D.; Lykoudis, P.; Raptis, R. G.; Mezei, G. Phosphonopolycarboxylates as chemical additives for calcite scale dissolution and metallic corrosion inhibition based on a calcium−phosphonotricarboxylate organic−inorganic hybrid. *Cryst. Growth Des.* **2006**, *6*, 1064–1067. (g) Barouda, E.; Demadis, K. D.; Freeman, S.; Jones, F.; Ogden, M. I. Barium sulfate crystallization in the presence of variable chain length aminomethylenetraphosphonates and cations (Na^+ or Zn^{2+}). *Cryst. Growth Des.* **2007**, *7*, 321–327. (h) Kofina, A. N.; Demadis, K. D.; Koutsoukos, P. G. The effect of citrate and phosphocitrate on struvite spontaneous precipitation. *Cryst. Growth Des.* **2007**, *7*, 2705–2712. (i) Akyol, E.; Öner, M.; Barouda, E.; Demadis, K. D. Systematic structural determinants of the effects of tetraphosphonates on gypsum crystallization. *Cryst. Growth Des.* **2009**, *9*, 5145–5154.

(5) Demadis, K. D. Neofotistou, E.; Mavredaki, E.; Stathoulopoulou, A. *Proceedings of the 10th European Symposium on Corrosion and Scale Inhibitors (10 SEIC)*; Ann. Univ. Ferrara, N.S., Sez. V, Suppl. N. 12, 2005; p 451.

(6) Demadis, K. D. Recent developments in controlling silica and magnesium silicate in industrial water systems. In *Science and Technology of Industrial Water Treatment*; CRC Press: London, 2010; Chapter 10, pp 179−203.

(7) (a) Simsek, S.; Yildirim, N.; Gulgor, A. Developmental and environmental effects of the Kizildere geothermal power project, Turkey. *Geothermics* **2005**, *34*, 234–251. (b) Sheikholeslami, R. Scaling of process equipment by saline streams - challenges ahead. *Water Sci. Technol.* **2004**, *49*, 201–210.

(8) http://www.ospar.org (accessed August 10, 2011).

(9) Demadis, K. D.; Mavredaki, E.; Somara, M. Additive-driven dissolution enhancement of colloidal silica. 1. Basic principles and relevance to water treatment. *Ind. Eng. Chem. Res.* **2011**, *50*, 12587–12595.

(10) Demadis, K. D.; Mavredaki, E. Green additives to enhance silica dissolution during water treatment. *Environ. Chem. Lett.* **2005**, *3*, 127–131.

(11) Miltenberger, K. Hydroxycarboxylic acids, aliphatic. In *Ullmann's Encyclopedia of Industrial Chemistry*; Wiley-VCH: Weinheim, 2005; DOI: 10.1002/14356007.a13_507.

(12) Davies, M. B.; Austin, J.; Partridge, D. A. *Vitamin C: Its Chemistry and Biochemistry*; The Royal Society of Chemistry: London, 1991; p 48.

(13) Hu, Y.-Y.; Rawal, A.; Schmidt-Rohr, K. Strongly bound citrate stabilizes the apatite nanocrystals in bone. *Proc. Natl. Acad. Sci. U.S.A.* **2010**, *107*, 22425–22429.

(14) (a) Johannsen, F. R. Toxicological profile of carboxymethyl inulin. *Food Chem. Toxicol.* **2003**, *41*, 49–59. (b) Coudray, C.; Demigné, C.; Rayssiguier, Y. Effects of dietary fibers on magnesium absorption in animals and humans. *J. Nutr.* **2003**, *133*, 1–4.

(15) Lin, H. H.; Chen, J. H.; Huang, C. C.; Wang, C. J. Apoptotic effect of 3,4-dihydroxybenzoic acid on human gastric carcinoma cells involving JNK/p38 MAPK signaling activation. *Int. J. Cancer* **2007**, *120*, 2306–2316.

(16) Ly, T. N.; Hazama, C.; Shimoyamada, M.; Ando, H.; Kato, K.; Yamauchi, R. Antioxidative compounds from the outer scales of onion. *J. Agric. Food Chem.* **2005**, *53*, 8183–8189.

(17) (a) Benes, F. M. Carlsson and the discovery of dopamine. *Trends Pharmacol. Sci.* **2001**, *22*, 46–47. (b) http://www.drugbank.ca/drugs/DB00988.

(18) Schwarzenbach, G. Der chelateffekt. *Helv. Chim. Acta* **1952**, *35*, 2344–2359.

(19) (a) Kopple, J. D.; Swendseid, M. E. Evidence that histidine is an essential amino acid in normal and chronically uremic man. *J. Clin. Invest.* **1975**, *55*, 881–891. (b) Benevenga, N. J.; Steele, R. D. Adverse-effects of excessive consumption of amino-acids. *Annu. Rev. Nutr.* **1984**, *4*, 157–181.

(20) Sprenger, G. A. Aromatic amino acids. Amino acid biosynthesis: pathways, regulation and metabolic engineering. Springer: New York, 2007; pp 106−113.

(21) (a) Coradin, T.; Eglin, D.; Livage, J. The silicomolybdic acid spectrophotometric method and its application to silicate/biopolymer interaction studies. *Spectroscopy* **2004**, *18*, 567–576. (b) Alexander, G. B. The reaction of low molecular weight silicic acids with molybdic acid. *J. Am. Chem. Soc.* **1953**, *75*, 5655–5657. (c) Truesdale, V. W.; Smith, P. J.; Smith, C. J. Kinetics of α-molybdosilicic and β-molybdosilicic acid formation. *Analyst* **1979**, 897–918. (d) Truesdale, V. W.; Smith, C. J. Spectrophotometric characteristics of aqueous solutions of α-molybdosilicic and β-molybdosilicic acids. *Analyst* **1975**, 797–805. (e) Truesdale, V. W.; Smith, C. J. Formation of molybdosilicic acids from mixed solutions of molybdate and silicate. *Analyst* **1975**, 203–212.

(22) (a) Demadis, K. D. Water treatment's "Gordian knot". *Chem. Process.* **2003**, *66* (5), 29–32. (b) Chen, H.-X.; Ma, X.-H.; Bo, S.-S.; Chen, J.-B. Preparation of Fe/Cr doped SiO_2 thin film on 304 stainless steel substrate originated from corrosion. *Corr. Eng., Sci. Technol.* **2011**, *46*, 453–457. (c) Zheng, S. X.; Li, J. H. Inorganic-organic sol gel hybrid coatings for corrosion protection of metals. *J. Sol-Gel Sci. Technol.* **2010**, *54*, 174–187.

(23) Fink, D. W.; Stong, J. D. The electronic spectral properties of gallic acid. *Spectrochim. Acta* **1982**, *38A*, 1295–1298.

(24) (a) André, E.; Lapouge, C.; Cornard, J.-P. Metal complexation of protocatechuic acid and its derivatives: determination of the optimal computational conditions for the simulation of electronic spectra. *THEOCHEM* **2007**, *806*, 131–140. (b) André, E.; Cornard, J.-P.; Lapouge, C. Characterization of the Al(III) binding site of protocatechuic acid by electronic spectroscopy and quantum chemical calculations. *Chem. Phys. Lett.* **2007**, *434*, 155–159.

(25) (a) Mohammed-Ziegler, I.; Billes, F. Vibrational spectroscopic calculations on pyrogallol and gallic acid. *THEOCHEM* **2002**, *618*, 259–265. (b) Fazary, A. E.; Taha, M.; Ju, Y.-H. Iron complexation studies of gallic acid. *J. Chem. Eng. Data* **2009**, *54*, 35–42.

(26) Demadis, K. D.; Papadaki, M.; Raptis, R. G.; Zhao, H. Corrugated, sheet-like architectures in layered alkaline earth metal R,S-hydroxy-phosphonoacetate frameworks: Applications for anti-corrosion protection of metal surfaces. *Chem. Mater.* **2008**, *20*, 4835–4846.

(27) Ehrlich, H.; Demadis, K. D.; Koutsoukos, P. G.; Pokrovsky, O. Modern views on desilicification: biosilica and abiotic silica dissolution in natural and artificial environments. *Chem. Rev.* **2010**, *110*, 4656–4689.

(28) Blesa, M. A.; Weisz, A. D.; Morando, P. J.; Salfity, J. A.; Magaz, G. E.; Regazzoni, A. E. The interaction of metal oxide surfaces with complexing agents dissolved in water. *Coord. Chem. Rev.* **2000**, *196*, 31–63.

(29) Rao, V. S.; Babu, S. M.; Ranganathan, S. Biocompatible small molecules that enhance silica solubilization under ambient conditions: Chemical profile of such complexes, possible mechanism for enhancement, and their effect on the growth and protection from pests in the rice plant (*Oryza sativa L.*). *Phosphorus Sulfur Silicon* **2009**, *184*, 1975–1990.

(30) Ma, J. F.; Tamai, K.; Yamaji, N.; Mitani, N.; Konishi, S.; Katsuhara, M.; Ishiguro, M.; Murata, Y.; Yano, M. A silicon transporter in rice. *Nature* **2006**, *440*, 688–691.

(31) Bai, S. Q.; Tsuji, Y.; Okaue, Y.; Yokoyama, T. First detection of a silicic acid complex with a catechol derivative under natural conditions. *Chem. Lett.* **2008**, *37*, 1168–1169.

(32) Bai, S.; Tsuji, Y.; Okaue, Y.; Yokoyama, T. Complexation of Silicic Acid with Tiron in Aqueous Solution Under near Natural Condition. *J. Solution Chem.* **2011**, *40*, 348–356.

(33) Araujo, P. Z.; Morando, P. J.; Blesa, M. A. Interaction of catechol and gallic acid with titanium dioxide in aqueous suspensions. 1. Equilibrium studies. *Langmuir* **2005**, *21*, 3470–3474.

(34) (a) Neofotistou, E.; Demadis, K. D. Silica scale growth inhibition by polyaminoamide STARBURST dendrimers. *Colloids Surf., A.* **2004**, *242*, 213–216. (b) Neofotistou, E.; Demadis, K. D. Use of antiscalants for mitigation of silica (SiO_2) fouling and deposition: fundamentals and applications in desalination systems. *Desalination* **2004**, *167*, 257–272. (c) Demadis, K. D. A structure/function study of polyaminoamide (PAMAM) dendrimers as silica scale growth inhibitors. *J. Chem. Technol. Biotechnol.* **2005**, *80*, 630–640. (d) Demadis, K. D.; Neofotistou, E.; Mavredaki, E.; Tsiknakis, M.; Sarigiannidou, E.-M.; Katarachia, S. D. Inorganic foulants in membrane systems: Chemical control strategies and the contribution of "green chemistry". *Desalination* **2005**, *179*, 281–295. (e) Demadis, K. D.; Stathoulopoulou, A. Solubility enhancement of amorphous silica with polyamine/polyammonium cationic macromolecules: relevance to silica laden process waters. *Ind. Eng. Chem. Res.* **2006**, *45*, 4436–4440. (f) Demadis, K. D.; Stathoulopoulou, A. Novel, multifunctional, environmentally friendly additives for effective control of inorganic foulants in industrial water and process applications. *Mater. Perform.* **2006**, *45* (1), 40–44. (g) Mavredaki, E.; Neofotistou, E.; Demadis, K. D. Inhibition and dissolution as dual mitigation approaches for colloidal silica (SiO_2) fouling and deposition in process water systems: functional synergies. *Ind. Eng. Chem. Res.* **2005**, *44*, 7019–7026. (h) Mavredaki, E.; Stathoulopoulou, A.; Neofotistou, E.; Demadis, K. D. Environmentally benign chemical additives in the treatment and chemical cleaning of process water systems: Implications for green chemical technology. *Desalination* **2007**, *210*, 257–265. (i) Ketsetzi, A.; Stathoulopoulou, A.; Demadis, K. D. Being "green" in chemical water treatment technologies: Issues, challenges and developments. *Desalination* **2008**, *223*, 487–493. (j) Demadis, K. D.; Neofotistou, E. Synergistic effects of combinations of cationic polyaminoamide dendrimers/anionic polyelectrolytes on amorphous silica formation: a bioinspired approach. *Chem. Mater.* **2007**, *19*, 581–587. (k) Demadis, K. D.; Ketsetzi, A.; Pachis, K.; Ramos, V. M. Inhibitory effects of multicomponent, phosphonate-grafted, zwitter-ionic chitosan biomacromolecules on silicic acid condensation. *Biomacromolecules* **2008**, *9*, 3288–3293. (l) Demadis, K. D.; Pachis, K.; Ketsetzi, A.; Stathoulopoulou, A. Bioinspired control of colloidal silica *in vitro* by dual polymeric assemblies of zwitterionic phosphomethylated chitosan and polycations or polyanions. *Adv. Colloid Interface Sci.* **2009**, *151*, 33–48. (m) Spinde, K.; Pachis, K.; Antonakaki, I.; Brunner, E.; Demadis, K. D. The influence of polyamines and related macromolecules on silicic acid polycondensation: relevance to "soluble silicon pools"? *Chem. Mater.* **2011**, *23*, 4676–4687.